2024 European Control Conference (ECC)
June 25-28, 2024. Stockholm, Sweden

Fast Charging of Li-ion Batteries via Learning and Optimization

Renato Rodriguez[1], Yan Wang[2], Damoon Soudbakhsh[1]

Abstract— **Complex electrochemical processes of Li-ion batteries result in nonlinear and high-dimensional dynamics. With the increased presence in critical applications, there is a demand for advanced fast-charging strategies to reduce the charging time while maximizing the battery's lifespan. Fast charging is limited by several factors, such as elevated temperature, since they accelerate electrochemical aging and, in turn, result in increased lithium plating, higher mechanical stresses, and an increased growth rate of the solid-electrolyte interface layer. Here, we propose an aggressive but efficient charging strategy using an adaptive control strategy that learns the closed-loop system's Jacobian from input/output data and optimizes the response based on the learned dynamics. To avoid subjecting the cell to accelerated aging, we optimize the electrical current for minimum battery charge time while respecting constraints such as maximum cell temperature and voltage. The battery data was generated using the Doyle-Fuller-Newman (P2D) model with a thermal model to characterize the cell's thermal effects. Our optimized charging strategy is comprised of a hybrid (mixed continuous-discrete) solution that fully charges a 5Ah 21700 NMC-811 cylindrical cell, 66% faster than the recommended 0.3C constant-current constant-voltage strategy while respecting safety constraints, including a maximum voltage of 4.2V and a maximum temperature of 57$^{\circ}C$.**

I. INTRODUCTION

This research presents a novel fast-charging strategy while maximizing the life of Li-ion batteries (LiBs) through learning and optimization of the electrical current input.

Over the last decade, LiBs have become the technology of choice for grid storage, portable electronics, and specifically electric vehicles (EVs). However, despite advancements in battery technology and incentives like tax credits, EV adoption still faces a major hurdle in slow charging times. Charging an EV battery pack to full capacity takes significantly longer than refueling a conventional vehicle [1]. This has led to increased demand for enhanced battery technologies that deliver fast-charging protocols with minimal charging duration while ensuring safety during operation.

The cycle life of lithium-ion batteries is significantly affected by the selected charging protocol [2]. Furthermore, fast charging can accelerate battery degradation. Thus, a trade-off exists between charging speed and battery lifespan [3]. The primary risk comes from subjecting the battery to high C-rates and the elevated temperatures that a fast charge generates [4]. Elevated temperatures can accelerate electrochemical aging, resulting in increased lithium plating, higher mechanical stresses, and an increased rate-of-growth of the SEI (solid-electrolyte interface) layer [5], [6].

The fast charging problem has been explored through various methods, including passive charging strategies, such as constant-current (CC), CC constant-voltage (CC-CV) [4], multi-stage CC-CV [7], and pulse charging techniques [5]; and through active optimal charging protocols. Passive charging techniques are model-free methods that characterize their predefined charging profiles with current, voltage, or power constraints. These methods, however, ignore the battery's response and thus are considered heuristic [1]. This has prompted the investigation of active optimal charging protocols to fulfill fast charging demands while mitigating their adverse effects on battery health.

Active optimal charging can be split into two categories. The first category uses empirical battery models such as equivalent circuit models (ECMs) [8] or machine learning models [9] to predict battery states using past measured data and state observers such as Kalman filters [10], or moving horizon estimators [11] to estimate the true/internal battery states. Also, it includes a control or optimization scheme, such as linear quadratic control [12], Pontryagin's minimum principle [13], or model predictive control (MPC) [14], [15], to improve charging performance. A significant body of literature employs MPC to address the optimal charging problem. This problem is framed as a constraint-based optimization whose goal is to either minimize the time required to reach a specific state of charge (SOC) or maximize the SOC achieved within a set charging duration. However, this technique is known for its computational intensity. Furthermore, real-time implementations often use empirical models, which are unable to reflect physics-based parameters and compromise the physical precision of the solution [14]. The second category of optimal charging strategies involves using physics-based models for calculating the battery states. These methods often utilize an MPC control scheme along with reduced-order methods such as the single-particle model (SPM) [16], and electrochemical models with a constant electrolyte concentration [17] since they experience reduced computational complexity when compared to full-order alternatives. This approach allows for formulating a closed-loop optimization problem to minimize charging time and can more naturally include physics-based constraints. Nonetheless, its efficacy is hampered by model inaccuracies stemming from the simplified representation of the battery dynamics, alongside its considerable computational complexity. Moreover, the streamlined dynamics fail to exploit the system's capabilities, potentially resulting in a conservative or infeasible solution depending on the problem formulation.

*This work was supported in part by the Office of Naval Research, Grant number N000142312612.

[1]R. Rodriguez and D. Soudbakhsh (corresponding author) are with the Dynamical Systems Lab (DSLab), Department of Mechanical Engineering, Temple University, Philadelphia, PA, USA {renato.rodriguez, damoon.soudbakhsh}@temple.edu

[2]Yan Wang is Retired Ford Motor Company, Dearborn, MI 48124.

This study proposes optimizing the charging profile (electrical current) for minimum battery charge time while respecting constraints, including a maximum cell temperature and a maximum voltage. This approach involves an adaptive learning and control strategy that learns the Jacobian of a closed-loop system from input/output data and optimizes the response based on the learned dynamics [18]–[20]. The primary benefit of employing this approach lies in the flexibility it offers to utilize full-order dynamics. The battery data was generated using the full-order electrochemical Doyle-Fuller-Newman (DFN, aka P2D) model [21], which is governed by porous electrode and concentrated solution theories. We also employ a thermal model that uses an energy balance approach to characterize the cell's thermal effects [22], making our electrochemical-thermal-based control law close to the actual battery mechanism. Our approach implements the hybrid (mixed continuous-discrete) framework, which aims to initially maximize current and subsequently dynamically transition between operating modes to meet constraints. Furthermore, our optimization approach initializes with information from a known solution (e.g., CC-CV). It optimizes a set of control points [23] (waveform parameters) to yield a charging strategy that meets fast charging demands and sustains the safe operation of a LiB system.

The key contributions of this research are i) adaptive learning and optimization for the lithium-ion battery's complex nonlinear dynamics, ii) including physical constraints in the optimization problem, iii) fast charging optimization of the system through direct data-driven control, and iv) validation of the optimal solutions using a high-fidelity full-order electrochemical-thermal battery simulator. Additionally, the presented approach can be adapted for constrained-based optimization of other complex dynamical systems.

II. Electrochemical Model And Battery Simulation

Here we describe the electrochemical model, Doyle-Fuller-Newman (DFN) model, used as the process dynamics in §II-A and present the battery simulation process via the Python Battery Mathematical Modelling (PyBaMM) package in §II-B.

A. Full-Order Electrochemical Model

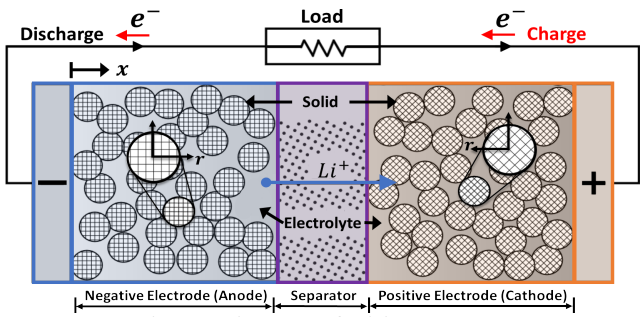

Fig. 1: Diagram of Li-ion Battery.

DFN is a comprehensive electrochemical lithium-ion battery model that characterizes the battery's internal operations using the principles of porous electrode and concentrated solution theories [24]. The model comprises a separator and two electronically isolated porous electrodes (anode and cathode), as shown in Figure 1. Lithium exists in solid and liquid phases. In the solid phase, a diffusion process within the active material moves lithium ions along the r-axis through the solid-electrolyte interface via Butler-Volmer kinetics. In the liquid phase, ions in the electrolyte travel through the separator along the x-axis to reach the opposite electrode [25]. A combination of ordinary differential equations (ODEs) and partial differential equations (PDEs) are used to describe the internal dynamics of the battery, encompassing electrochemical kinetics, diffusion, and intercalation. The DFN model uses the following state variables including the electric potential in the electrolyte ($\phi_e(x,t)$) and the solid phase ($\phi_s^{\pm}(x,t)$), the concentration of lithium in the electrolyte ($c_e(x,t)$) and the solid phase ($c_s^{\pm}(x,r,t)$), the ionic current in the electrolyte ($i_e^{\pm}(x,t)$), and the flux density between the solid phase and electrolyte ($j_n^{\pm}(x,t)$).

The physical model takes as an input the applied current $I(t)$ and yields the voltage across the current collectors $V(t)$ as the model output. The model output is represented by:

$$V(t) = \phi_s^{+}(0^{+},t) - \phi_s^{-}(0^{-},t). \tag{1}$$

The battery's available energy can be determined by the volume-averaged solid-phase lithium concentration in the anode [15]. This calculation assumes the anode capacity to be the limiting factor and yields the SOC calculation as follows:

$$\text{SOC}(t) = 100\left[\frac{\left(\frac{1}{L^{-}c_{s,max}^{-}}\int_0^{L^{-}} c_{s,avg}^{-}(x,t)dx\right) - \theta_{min}}{\theta_{max}-\theta_{min}}\right], \tag{2}$$

where $c_{s,avg}^{-}$ represents the volume-averaged solid phase concentration in each solid particle in the anode, $c_{s,max}^{-}$, represents the maximum solid phase concentration in the anode, L^{-} represents the anode length, and θ_{max} and θ_{min} represent the SOC at the fully charged/discharged states, respectively. We note that these parameters are defined by the anode's stoichiometric limits.

Additionally, the standard DFN model is extended with a thermal model that couples the porous electrode theory with an energy conservation approach to describe the cell's thermal behavior, including Ohmic heating in both the solid and the electrolyte, as well as reversible and irreversible heating resulting from electrochemical reactions [22]. The spatially averaged cell temperature ($\bar{T}$) is given by:

$$\bar{T}(t) = \frac{1}{L}\int_0^{L} T(x,t)dx, \tag{3}$$

This representation is justified since P2D models often have negligible temperature variation in the cell [26].

B. Battery Simulations

We employed the Python Battery Mathematical Modeling (PyBaMM) framework [27] for efficient battery simulations. This framework solves electrochemical differential equations using differential and numerical solvers. PyBaMM follows a

"plug-and-play physics" methodology, facilitating the integration of thermal effects into battery models [22].

In this study, we adopt the battery chemistry found in a commercial LGM50 21700 cylindrical cell. This specific cell boasts a 5 Ah capacity, with Nickel Manganese Cobalt Oxide (NMC) 811 as the positive electrode and a bi-component Graphite (SiO_x) as the negative electrode [28]. We used the PyBaMM-DFN model for the calculation of relevant battery outputs, such as voltage V, state-of-charge SOC, and temperature T, for a selected electrical current I input (e.g., CC-CV, pulse charging techniques, etc.). The battery simulation and data collection process is shown in Fig. 2. We note that the battery simulations initialize the battery SOC to 0% and use an ambient/initial-cell temperature of 25^oC.

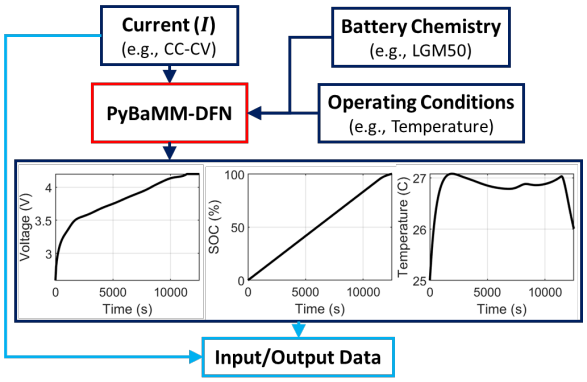

Fig. 2: Schematic of Data Collection Process.

III. Adaptive Learning Optimization

Here, we developed a Jacobian learning method. This method allows for optimizing the charging profile with simulated battery response data from the full-order electrochemical model to prevent subjecting the battery to unsafe operating conditions. The existence of the solutions is guaranteed as the optimizer initializes with a sub-optimal baseline solution (e.g., CC-CV), and the adaptive learning optimizer enhances the previous solution at each iteration.

A. Problem Formulation

We assume that the complex nonlinear lithium-ion battery systems have the following general form:

$$\dot{x} = f(x, u). \tag{4}$$

where x represents the states and u represents the inputs. The goal is to find an optimal input (charging profile), u^*, that maximizes SOC within a set charging duration. The general formulation of the optimization criteria is given by:

$$u^* = \arg\min_{u \in U} \int_0^{t_f} \varphi(x(t), u(t), t)dt \tag{5}$$

subject to the constraints:

$$u_{lb} \leq u(t) \leq u_{ub}$$
$$x_{lb} \leq x(t) \leq x_{ub}$$

where the constraints are defined by lower and upper bounds on the inputs (u_{lb}, u_{ub}) and the states (x_{lb}, x_{ub}), respectively. The constraints include i) bounds on the electrical current input and ii) limitations on the state variables for safe LiB operation, such as a maximum and minimum battery voltage and a maximum temperature. These constraints are summarized in Table I. We note that the specific optimization criteria and constraints depend on the specific battery and the desired charging strategy. Furthermore, our method is amenable to changes, e.g., other criteria and constraints.

	Optim. Criteria / Constraints
SOC [%]	Maximize value at t_f
SOC_d [%]	100% (fully charged)
Temperature [^oC]	maximum: 57
Voltage [V]	maximum: 4.2 minimum: 2.5
Current [C-rate]	maximum: 2.5 minimum: 0

TABLE I: Optimization Criteria and Constraints

B. Jacobian Learning Optimization

This section outlines the methodology of Jacobian learning (JL), an adaptive optimization approach. JL employs learning techniques to identify and recursively update the system's input/output sensitivity. It is leveraged to discern the dominant characteristics of the target system using input-output data, enabling model-free control of complex systems.

The Jacobian learning process is executed through a recursive least squares approach [20]. After this process is completed and the Jacobian (input-output sensitivity) is acquired, it is applied with a gradient-descent optimization strategy to perform constrained optimizations of the inputs. The optimization process contains two sequential steps: the first step entails conducting a full continuous-time simulation, while the second step (discrete time) utilizes insights from the first step to map out the subsequent simulation [19], [29]. This iterative process persists until the optimization metric (e.g., SOC) converges to the optimal solution or until a predefined maximum iteration limit is reached.

a) JL Problem Formulation

Here, we introduce a category of static models frequently encountered in various slow processes or in systems that exhibit dynamics that can be disregarded in relation to the sampling rate. These models are assumed to be zero-order and are nonlinear but smooth [20]. As depicted in Fig. 3, the desired output y_d is attained through an iterative optimization of the inputs u to the plant, based on a data-driven model (Jacobian) developed from measurements of the inputs u and outputs y. An overview of the methodology is given below.

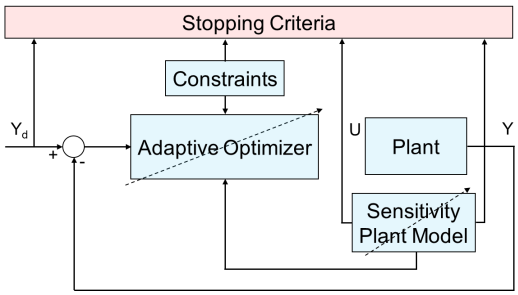

Fig. 3: Diagram of the Learning and Optimization Algorithm

We assume the inputs $u[k]$ and outputs $y[k]$ to be related

with a static nonlinearity

$$y[k] = S(u[k]) \tag{6}$$

where $S(u[k])$ is a nonlinear and smooth function. Here, the controller aims to minimize the error, $e[k]$, between the system output, $y[k]$, and the desired output,y_d, by optimizing the input vector $u[k]$. The error is given by:

$$\|e[k]\|_2 = \|y[k] - y_d[k]\|_2, \tag{7}$$

where $y_d[k]$ is the desired output vector at time k.

Next, we discuss the recursive least squares approach for learning the Jacobian $\mathbb{J}[k]$ and recursively updating it to maintain the learned sensitivity. First, we consider a linearized time-varying approximation of the mapping S:

$$\Delta y[k] = \mathbb{J}[k]\Delta u[k] \tag{8}$$

where,

$$\begin{aligned} \Delta u[k] &= u[k] - u[k-1] \quad , \qquad \Delta u[k] \in R^r \\ \Delta y[k] &= y[k] - y[k-1] \quad , \qquad \Delta y[k] \in R^q \end{aligned} \tag{9}$$

and r and q represent the number of inputs and outputs, respectively. We note, for multi-output systems ($q > 1$), (8) is decompose into q single-output subsystems $\mathbb{J}_j[k]$:

$$\Delta y_j[k] = \mathbb{J}_j[k]\Delta u[k] \tag{10}$$

where $j = 1, 2, ..., q$. The optimal input update for minimizing the cost in (7) when the Jacobian $\mathbb{J}[k]$ is known can be found from (8) using the pseudo-inverse $\mathbb{J}^\dagger[k]$ as [19].

$$u[k+1] = u[k] + \mathbb{J}^\dagger[k](y_d[k] - y[k]) \tag{11}$$

To prevent singularities, we introduce regularization of $\mathbb{J}^\dagger[k]$ using $H[k]$ as:

$$\begin{aligned} H[k] &= \mathbb{J}^T[k](\mathbb{J}[k]\mathbb{J}^T[k] + \rho I_q)^{-1} \quad \text{for} \quad r \geq q \\ H[k] &= (\mathbb{J}^T[k]\mathbb{J}[k] + \rho I_q)^{-1}\mathbb{J}^T[k] \quad \text{for} \quad r \leq q \end{aligned} \tag{12}$$

where I_q is the $q \times q$ identity matrix and ρ is a small positive constant ($\rho \in (0, 1)$). However, often, the Jacobian is unknown and must be estimated. Once learned, the estimated Jacobian $\widehat{\mathbb{J}}$ can be used as a feedback control law of the form:

$$u[k+1] = u[k] + \widehat{H}[k]G(y_d - y[k]) \tag{13}$$

where G represents the control gains with its diagonal elements as $g_i \in (0, 2)$. If $r \leq q$, $\widehat{H}[k]$ is defined as:

$$\widehat{H}[k] = (\widehat{\mathbb{J}}^T[k]\widehat{\mathbb{J}}[k] + \rho I_q)^{-1}\ G\ \widehat{\mathbb{J}}^T[k] \tag{14}$$

Here, we employ an adaptive learning approach to find and recursively update the Jacobian to account for Jacobian changes in time, which can be represented by:

$$\mathbb{J}_j[k+1] = \mathbb{J}[k] + w_j[k], \tag{15}$$

$$\Delta y_j[k] = \Delta u^T[k]\mathbb{J}_j[k] + v_j[k],\ j = [1, q], \tag{16}$$

where the vector $w_j[k]$ signifies the process noise while $Q_j = E\{w_j^T[k]w_j[k]\}$ denotes the expected covariance of the model's imprecision, and $v_j[k]$ characterizes the measurement noise while $R_j = E\{v_j^2[k]\}$ represents the expected variance of the measurement noise [29]. Further, the Jacobian of each simplified subsystems (10) can be estimated as:

$$\widehat{\mathbb{J}}_j^T[k] = \widehat{\mathbb{J}}_j^T[k-1] + \frac{P_j[k-1]\Delta u[k](\Delta y[k] - \widehat{\mathbb{J}}_j[k-1]\Delta u[k])}{R_j + \Delta u^T[k]P_j[k-1]\Delta u[k]} \tag{17}$$

$$P_j[k] = P_j[k-1] - \frac{P_j[k-1]\Delta \mathrm{u}[k]\Delta u^T[k]P_j[k-1]}{R_j + \Delta u^T[k]P_j[k-1]\Delta u[k]} + Q_j. \tag{18}$$

To accommodate for constraints, the optimal feedback control law (13) can be reformulated as a constraint-based optimization problem given by:

$$u^*[k] = \underset{u[k]}{\arg\min}(\|y_d - \widehat{y}[k]\|^2 + \gamma\|u[k] - u[k-1]\|^2) \tag{19}$$

$$\text{s.t.} \qquad \widehat{y}[k] = y[k-1] + \widehat{\mathbb{J}}[k](u[k] - u[k-1]).$$

The update in (19) can be implemented through widely accessible quadratic programming solvers, such as Matlab's FMINCON and LSQLIN functions.

IV. Results

This section presents the optimal charging strategy synthesized with our adaptive learning and optimization method. Our approach employed a full-order electrochemical (DFN) model coupled with a thermal model for capturing the battery's thermal effects, making our electrochemical-thermal-based control law close to the actual battery mechanism.

We explored different charging strategies, including passive changing strategies in §IV-A. Our optimal results are presented in §IV-B along with a comparison to the other charging strategies.

A. Passive Charging Strategies

Passive charging techniques are model-free methods that charge the battery under preset instructions, as shown in Fig. 4. The charging profiles developed with these methods are characterized by their fixed terminal conditions, including current, voltage, or power constraints. However, passive charging algorithms do not consider the feedback of the battery states, which may lead to a shortened battery lifespan.

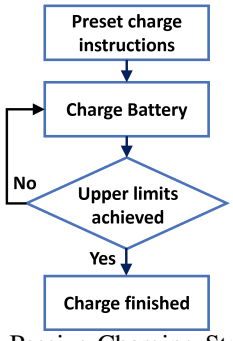

Fig. 4: Passive Charging Structure

A common and arguably most widely used charging strategy is constant-current constant-voltage (CC-CV) due to its easy implementation and operation. This algorithm initially charges the battery with a constant current until the voltage reaches a preset upper limit. Then, the voltage is held constant until the current is reduced to a preset minimum

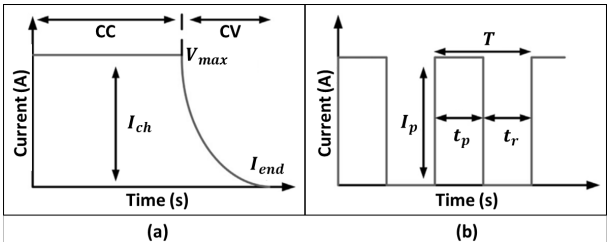

Fig. 5: Passive Charging Strategies: (a) CC-CV, (b) PPC

Strategy	Charge Time (s)	Max T (C)	Max V (V)
CC-CV: 0.3C	12,500	27	4.20
CC-CV: 2.0C	4,000	64	4.20
Hybrid:	4,000	57	4.22

TABLE II: Comparison of Charging Strategies

value. In this study, we tested the CC-CV charging protocol under different changing rates (C-rates) to fully charge a 5Ah 21700 NMC-811 cylindrical cell. First, we tested the conventional 0.3C CC-CV charging strategy following the battery manufacturer's specifications. Next, we tested a fast-charging 2C CC-CV charging protocol, which reduced the charging time to around 4000 seconds from the 12000 seconds needed to fully charge the cell with the 0.3C CC-CV. However, this reduction in time came with a substantial rise in the battery's temperature, surpassing the maximum temperature of $63°C$. Moreover, subjecting the battery to elevated temperatures can lead to adverse effects on battery health, such as accelerated electrochemical aging [5], [6]. The CC-CV charging protocols are baselines for comparison against our constrained-based optimal solution, which aims to fulfill fast charging demands while maintaining safe operating conditions by respecting constraints. The corresponding plots and the summarized results are presented in §IV-B.

B. Optimal Results

Here, we present the optimal charging profile developed with our adaptive optimization approach to maximize the battery SOC within a set charging duration (t_f) while respecting safety constraints. This is achieved by minimizing the square error between the SOC reached during the iteration and the desired SOC (SOC_d) of 100% (fully charged). The optimization objective and operational constraints are defined in (20) and summarized in Table I.

$$I^* = \arg\min_I \int_0^{t_f} (SOC(t) - SOC_d)^2 dt \qquad (20)$$

subject to the constraints:

$$T(t) \leq T_{ub}$$
$$V_{lb} \leq V(t) \leq V_{ub}$$
$$I_{lb} \leq I(t) \leq I_{ub}$$

Our optimized charging strategy comprises a hybrid (mixed continuous-discrete) solution, where continuous refers to the direct simulation of operating modes (e.g., CC, CV, pulse), and discrete refers to a transition between the operating modes. This approach aims to maximize current and subsequently dynamically transition between operating modes to meet constraints. Since the battery has a smaller resistance in the lower SOC range, the highest current is applied as a positive pulse current (PPC), whose waveform parameters (refer to Fig. 5) such as peak charging current (I_p), pulse on-time (t_p), relaxation interval time (t_r), and total pulse period (T) are optimized via our adaptive learning and control approach. Pulse charging was implemented, as it can be an efficient and fast charging strategy that, with proper selection of current waveform parameters, can help prevent the side reactions caused by saturation at the particle interface [30]. Following the PPC mode, the solution switches to CV to avoid continuing temperature rise due to the battery's rapidly increasing internal resistance.

Our optimization approach initializes with information (e.g., t_f, I_{ch}, I_{end}, etc.) from the 2C CC-CV profile. It optimizes a set of control points (PPC parameters) to yield a fast charge time while respecting safety constraints, including a maximum voltage of 4.2V and a maximum temperature of 57 $°C$ corresponding to 90% of the maximum surface temperature of $63°C$. The optimized charging strategy fully charged the 5Ah 21700 NMC-811 cylindrical cell, 66% faster than the recommended 0.3C CC-CV strategy. It maintained a temperature of $57°C$ or lower while the 2C CC-CV strategy experienced higher temperatures, reaching upwards of $64°C$. The results are summarized in Table II, while the plots are shown in Fig 6.

V. Conclusions

In this work, we developed a constrained optimal charging strategy that meets fast charging demands and sustains LiBs' safe operation. To avoid subjecting the cell to accelerated aging, we propose optimizing the electrical current for minimum battery charge time while respecting safety constraints, including a maximum cell temperature and a maximum voltage. We used a control strategy to learn the Jacobian of a closed-loop system from input/output data generated by a full-order electrochemical-thermal battery model. Based on the learned dynamics, we optimized the response. Our optimized charging strategy is comprised of a hybrid (mixed continuous-discrete) solution that fully charges a 5Ah 21700 NMC-811 cylindrical cell, 66% faster than the recommended 0.3C constant-current constant-voltage (CC-CV) strategy. Furthermore, it maintained a temperature of $57°C$ (90% of the $63°C$ maximum temperature) or lower while a comparable 2C CC-CV strategy experienced higher temperatures surpassing $63°C$, which can lead to adverse effects on battery health. Future work includes expanding our optimization criteria to include minimizing damage to the cyclable life of the battery quantified by capacity fade. Also, we plan on improving the efficiency of our optimization approach by substituting the complex electrochemical model with a high-fidelity, data-driven, reduced-order model.

Acknowledgements

This work was supported in part by the Office of Naval Research (ONR) under grant number N000142312612.

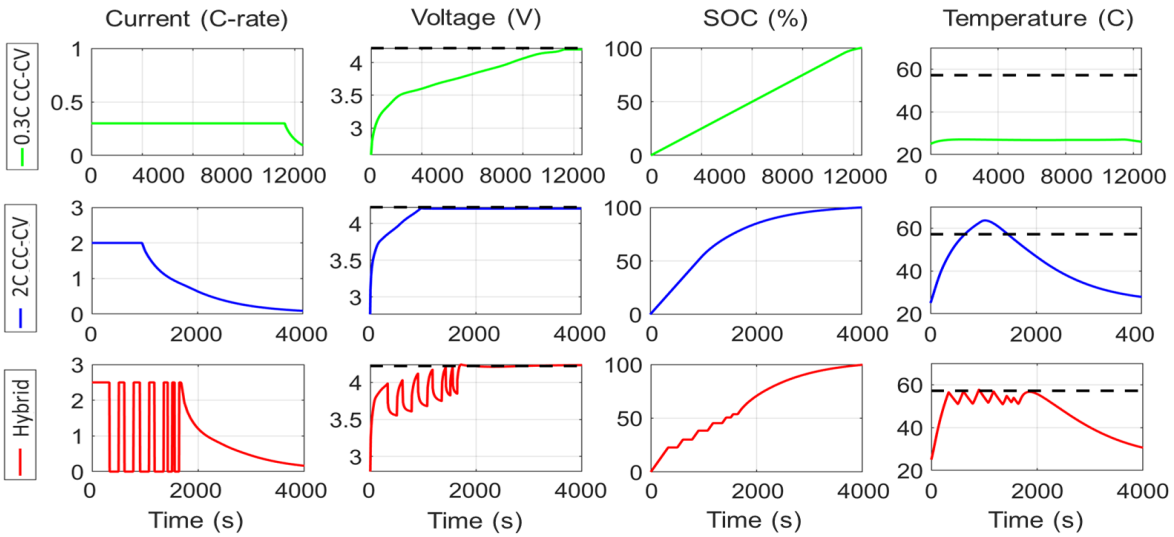

Fig. 6: Comparison of Charging Strategies

REFERENCES

[1] Y. Gao, X. Zhang, Q. Cheng, B. Guo, and J. Yang, "Classification and review of the charging strategies for commercial lithium-ion batteries," *Ieee Access*, vol. 7, pp. 43511–43524, 2019.

[2] S. Wang, C. Fernandez, Y. Chunmei, F. Yongcun, C. Wen, D.-I. Stroe, and Z. Chen, *Battery System Modeling*. Elsevier, 2021.

[3] C. Zhang, J. Jiang, Y. Gao, W. Zhang, Q. Liu, and X. Hu, "Charging optimization in lithium-ion batteries based on temperature rise and charge time," *Applied energy*, vol. 194, pp. 569–577, 2017.

[4] D. Anseán, M. Dubarry, A. Devie, B. Y. Liaw, V. M. García, J. C. Viera, and M. González, "Fast charging technique for high power LiFePO4 batteries: A mechanistic analysis of aging," *J. Power Sources*, vol. 321, pp. 201–209, 2016.

[5] A. Tomaszewska, Z. Chu, X. Feng, S. O'kane, X. Liu, J. Chen, C. Ji, E. Endler, R. Li, and L. Liu, "Lithium-ion battery fast charging: A review," *ETransportation*, vol. 1, p. 100011, 2019.

[6] M. D. Berliner, D. A. Cogswell, M. Z. Bazant, and R. D. Braatz, "A mixed continuous-discrete approach to fast charging of li-ion batteries while maximizing lifetime," *IFAC-PapersOnLine*, vol. 55, no. 30, pp. 305–310, 2022.

[7] M. U. Tahir, A. Sangwongwanich, D.-I. Stroe, and F. Blaabjerg, "Overview of multi-stage charging strategies for Li-ion batteries," *J. Energy Chem.*, 2023.

[8] D. Natella, S. Onori, and F. Vasca, "A Co-Estimation Framework for State of Charge and Parameters of Lithium-Ion Battery With Robustness to Aging and Usage Conditions," *IEEE Trans. Ind. Electron.*, vol. 70, pp. 5760–5770, June 2023.

[9] E. Chemali, P. J. Kollmeyer, M. Preindl, and A. Emadi, "State-of-charge estimation of Li-ion batteries using DNN: A machine learning approach," *J. Power Sources*, vol. 400, pp. 242–255, 2018.

[10] C. Campestrini, S. Kosch, and A. Jossen, "Influence of change in open circuit voltage on the state of charge estimation with an extended Kalman filter," *J. Energy Storage*, vol. 12, pp. 149–156, 2017.

[11] X. Hu, D. Cao, and B. Egardt, "Condition monitoring in advanced battery management systems: Moving horizon estimation using a reduced electrochemical model," *IEEE/ASME Trans. Mechatronics*, vol. 23, no. 1, pp. 167–178, 2017.

[12] H. Fang, Y. Wang, and J. Chen, "Health-aware and user-involved battery charging management for electric vehicles," *IEEE Trans. Control Syst. Technol.*, vol. 25, no. 3, pp. 911–923, 2016.

[13] S. Park, D. Lee, H. J. Ahn, C. Tomlin, and S. Moura, "Optimal control of battery fast charging based-on Pontryagin's minimum principle," in *IEEE Conference CDC'2020*, pp. 3506–3513, IEEE, 2020.

[14] G. Kujundžić, Šandor Ileš, J. Matuško, and M. Vašak, "Optimal charging of valve-regulated lead-acid batteries based on model predictive control," *Applied Energy*, vol. 187, pp. 189–202, 2017.

[15] S. Kolluri, S. V. Aduru, M. Pathak, R. D. Braatz, and V. R. Subramanian, "Real-time nonlinear model predictive control (NMPC) strategies using physics-based models for advanced lithium-ion battery management system (BMS)," *J. Electrochem. Soc.*, vol. 167, no. 6, p. 063505, 2020.

[16] J. Liu, G. Li, and H. K. Fathy, "An extended differential flatness approach for the health-conscious nonlinear model predictive control of lithium-ion batteries," *IEEE Trans. Control Syst. Technol.*, vol. 25, no. 5, pp. 1882–1889, 2016.

[17] R. Klein, N. A. Chaturvedi, J. Christensen, J. Ahmed, R. Findeisen, and A. Kojic, "Optimal charging strategies in lithium-ion battery," in *ACC'2021*, pp. 382–387, IEEE, 2011.

[18] R. Rodriguez, Y. Wang, J. Ozanne, D. Sumer, D. Filev, and D. Soudbakhsh, "Adaptive takeoff maneuver optimization of a sailing boat for america's cup," *J. Sail. Technol.*, vol. 7, no. 01, pp. 88–103, 2022.

[19] D. P. Filev, S. Bharitkar, and M.-F. Tsai, "Nonlinear control of static systems with unsupervised learning of the initial conditions," in *18th NAFIPS'1999 (Cat. No. 99TH8397)*, pp. 169–173, 1999.

[20] D. Soudbakhsh, A. M. Annaswamy, Y. Wang, S. L. Brunton, J. Gaudio, H. Hussain, D. Vrabie, J. Drgona, and D. Filev, "Data-Driven Control: Theory and Applications," in *ACC'2023*, pp. 1922–1939, 2023.

[21] R. Rodriguez, O. Ahmadzadeh, Y. Wang, and D. Soudbakhsh, "Data-Driven Discovery of Lithium-Ion Battery State of Charge Dynamics," *J. Dyn. Sys., Meas., Control.*, pp. 1–13, 2024.

[22] R. Timms, S. G. Marquis, V. Sulzer, C. P. Please, and S. J. Chapman, "Asymptotic reduction of a lithium-ion pouch cell model," *SIAM SIAP*, vol. 81, no. 3, pp. 765–788, 2021.

[23] R. Rodriguez, Y. Wang, J. Ozanne, J. Morrow, D. Sumer, D. Filev, and D. Soudbakhsh, "Adaptive learning and optimization of high-speed sailing maneuvers for america's cup," *J. Dyn. Sys., Meas., Control*, vol. 145, no. 2, p. 021005, 2023.

[24] R. Rodriguez, O. Ahmadzadeh, Y. Wang, and D. Soudbakhsh, "Discovering governing equations of li-ion batteries pertaining state of charge using input-output data," in *ACC'2023*, pp. 3081–3086, 2023.

[25] D. Luder, P. Caliandro, and A. Vezzini, "Enhanced physics-based models for state estimation of li-ion batteries," in *Proc. COMSOL Conf.*, 2020.

[26] S. Al Hallaj, H. Maleki, J.-S. Hong, and J. R. Selman, "Thermal modeling and design considerations of lithium-ion batteries," *J. Power Sources*, vol. 83, no. 1-2, pp. 1–8, 1999.

[27] V. Sulzer, S. G. Marquis, R. Timms, M. Robinson, and S. J. Chapman, "Python battery mathematical modelling (pybamm)," *J. Open Res. Softw.*, vol. 9, no. 1, 2021.

[28] C.-H. Chen, F. B. Planella, K. O'regan, D. Gastol, W. D. Widanage, and E. Kendrick, "Development of experimental techniques for parameterization of multi-scale lithium-ion battery models," *J. Electrochem. Soc.*, vol. 167, no. 8, p. 080534, 2020.

[29] R. Rodriguez, Y. Wang, J. Ozanne, D. Sumer, D. Filev, and D. Soudbakhsh, "Adaptive learning for maximum takeoff efficiency of high-speed sailboats," *IFAC-PapersOnLine*, vol. 55, no. 12, pp. 402–407, 2022.

[30] B. Purushothaman, P. Morrison, and U. Landau, "Reducing mass-transport limitations by application of special pulsed current modes," *J. Electrochem. Soc.*, vol. 152, no. 4, p. J33, 2005.